

STK4060

Time Series

OBLIG 1

Egil Furnes
Student: 693784

Exercise 1

(a)

We simulate a zero-mean Gaussian stationary process X_t with autocovariance $\gamma_X(h) = \rho^{|h|}$, where $\rho = 0.4$ and $n = 100$. The empirical autocovariances for lags 0, 1, 2, 3 are:

```
# A tibble: 4 × 2
  lag    empirical_autocov
  <int>          <dbl>
1     0            1.23
2     1            0.476
3     2            0.177
4     3            0.133
```

These are close to the theoretical values $\rho^h = (1, 0.4, 0.16, 0.064)$ up to sampling variability.

(b)

Now define $Y_t = \beta t + X_t$ with $\beta = 0.05$. Since βt is deterministic,

$$\text{Cov}(Y_t, Y_{t+h}) = \text{Cov}(X_t, X_{t+h}) = \rho^{|h|}.$$

The simulated time series Y_t is shown in Figure 1.

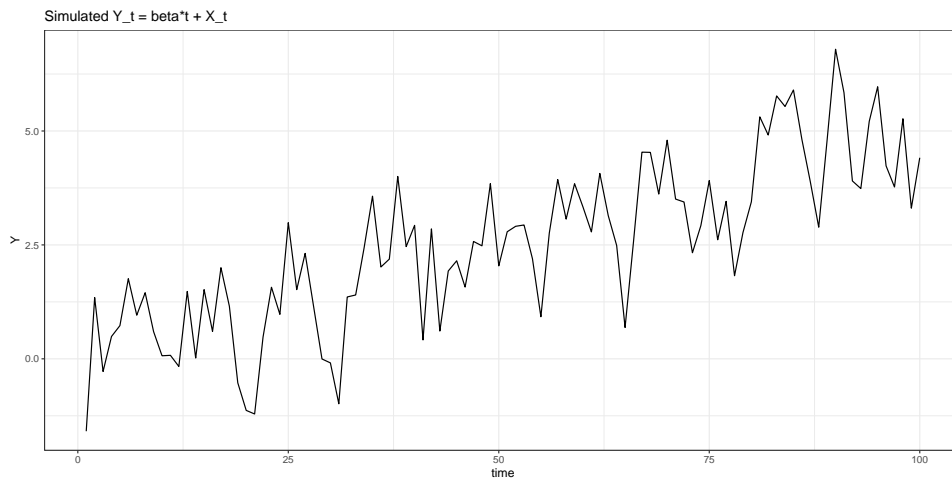


Figure 1: Sample path of $Y_t = \beta t + X_t$, $\beta = 0.05$, $\rho = 0.4$.

The empirical autocovariances are:

```
# A tibble: 4 × 2
  lag empirical_autocov_Y
  <int>          <dbl>
1     0            3.25
2     1            2.38
3     2            2.17
4     3            1.76
```

They are much larger than those of X_t , because the linear trend dominates the covariance.

(c)

For $Y_t = \mu_t + X_t$ with $\mu_t = \beta t$, the sample covariance satisfies

$$\mathbb{E}[\hat{\gamma}_Y(h)] \approx \underbrace{\frac{1}{n-h} \sum_{t=1}^{n-h} (\mu_t - \bar{\mu})(\mu_{t+h} - \bar{\mu})}_{\text{deterministic component}} + \rho^h.$$

The deterministic part is large and positive for a linear trend, explaining why the empirical values in (b) far exceed ρ^h . Using $\beta = 0.05$, $n = 100$:

```
# A tibble: 4 × 5
  lag empirical_autocov_Y deterministic_component gamma_X_theory
  <int>          <dbl>                  <dbl>          <dbl>
1     0            3.22                2.08           1
2     1            2.54                2.04           0.4
3     2            2.30                2.00           0.16
4     3            2.17                1.95           0.064
# 1 more variable: expected_gammahat_Y <dbl>
```

The observed values match the theoretical prediction (trend term) + ρ^h .

(d)

Because Y_t is not stationary due to the linear trend, the sample autocovariance in (b) was dominated by the deterministic component. A standard fix is to *detrend* the data. Since the trend is known to be $\mu_t = \beta t$, we define

$$Y_t^* = Y_t - \hat{\mu}_t = Y_t - \beta t$$

The empirical autocovariances of the detrended series are:

```
# A tibble: 4 × 2
  lag empirical_autocov_Ystar
  <int>             <dbl>
1     0            0.750
2     1            0.239
3     2           -0.108
4     3           -0.100
```

These values are of the same order of magnitude as the theoretical $\rho^h = (1, 0.4, 0.16, 0.064)$, up to sampling variation, and are dramatically smaller than the inflated covariances of Y_t in (b). The large artificial autocovariance caused by the linear trend disappears after detrending, and the behaviour again resembles that of the original stationary process X_t .

Exercise 2

(a)

A sample path from the stationary AR(1) with $\phi = 0.543$ and $W_t \sim \mathcal{N}(0, 1)$ is shown in Figure 2.

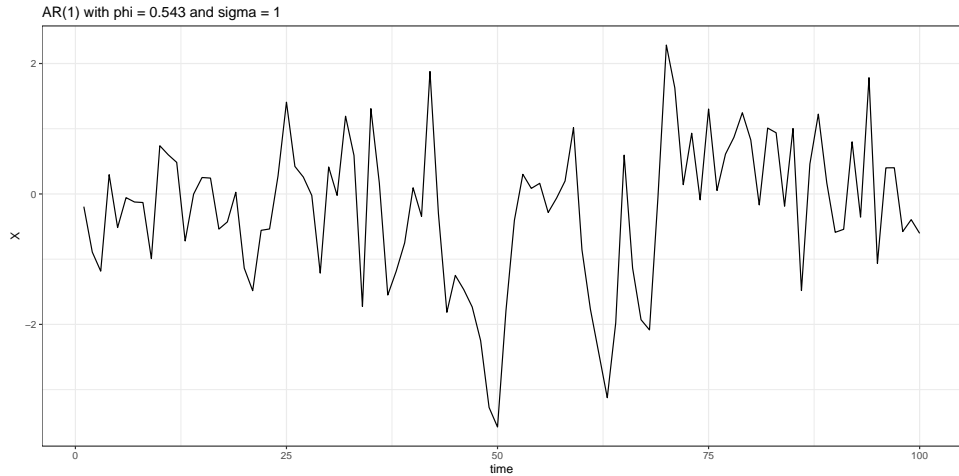


Figure 2: AR(1) with $\phi = 0.543$ and unit innovation variance.

(b)

For the causal AR(1) $X_t = \phi X_{t-1} + W_t$ with $W_t \stackrel{i.i.d.}{\sim} \mathcal{N}(0, 1)$ and stationary $X_1 \sim \mathcal{N}(0, (1 - \phi^2)^{-1})$, the log-likelihood is

$$\ell_n(\phi) = \frac{1}{2} \log(1 - \phi^2) - \frac{1}{2}(1 - \phi^2)x_1^2 - \frac{1}{2} \sum_{t=2}^n (x_t - \phi x_{t-1})^2.$$

The score and observed information (per $-1/n$) are

$$\frac{\partial}{\partial \phi} \ell_n(\phi) = -\frac{\phi}{1-\phi^2} + x_1^2 \phi + \sum_{t=2}^n (x_t - \phi x_{t-1}) x_{t-1}, \quad J_n = -\frac{1}{n} \frac{\partial^2}{\partial \phi^2} \ell_n(\phi).$$

Evaluated at the simulated sample,

$$\ell_n(0.543) = -50.28, \quad \frac{\partial}{\partial \phi} \ell_n(0.543) = -6.90, \quad J_n(0.543) = 1.348.$$

(c)

Since $|\phi| < 1$, $X_t = \sum_{k=0}^{\infty} \phi^k W_{t-k}$ and $\{X_t\}$ is stationary with $\text{Var}(X_t) = (1 - \phi^2)^{-1}$ and $\gamma(h) = \phi^{|h|}/(1 - \phi^2)$. Using Isserlis' formula, $\text{Cov}(X_t^2, X_{t+h}^2) = 2\gamma(h)^2$ is absolutely summable, hence by the ergodic theorem

$$\frac{1}{n} \sum_{t=1}^n X_t^2 \xrightarrow{p} (1 - \phi^2)^{-1}.$$

For the simulated data,

$$\frac{1}{n} \sum_{t=1}^n X_t^2 = 1.33,$$

which matches the theoretical value $(1 - \phi^2)^{-1} \approx 1.35$.

(d)

From (b),

$$J_n = \frac{1}{n} \left\{ \frac{1 + \phi^2}{(1 - \phi^2)^2} - x_1^2 + \sum_{t=1}^{n-1} x_t^2 \right\} \xrightarrow{p} \frac{1}{1 - \phi^2}.$$

Therefore

$$\sqrt{n} (\hat{\phi}_n - \phi) \xrightarrow{d} \mathcal{N}(0, 1 - \phi^2),$$

the same asymptotic limit as the least-squares estimator.

(e)

The Whittle estimator works in the frequency domain. After taking the Fourier transform, the periodogram values $|d_X(j/n)|^2$ behave almost like independent exponential variables with mean equal to the spectral density $f(j/n, \phi)$. So minimising

$$\ell_n^W(\phi) = - \sum_j \{ \log f(j/n, \phi) + |d_X(j/n)|^2 / f(j/n, \phi) \}$$

is just matching the model spectrum to the data. For AR(1) this gives an estimator that is asymptotically as good as exact ML, but much easier to compute.

(f)

Figure 3 shows $-\ell_n^W(\phi)$ on $\phi \in (-0.99, 0.99)$.

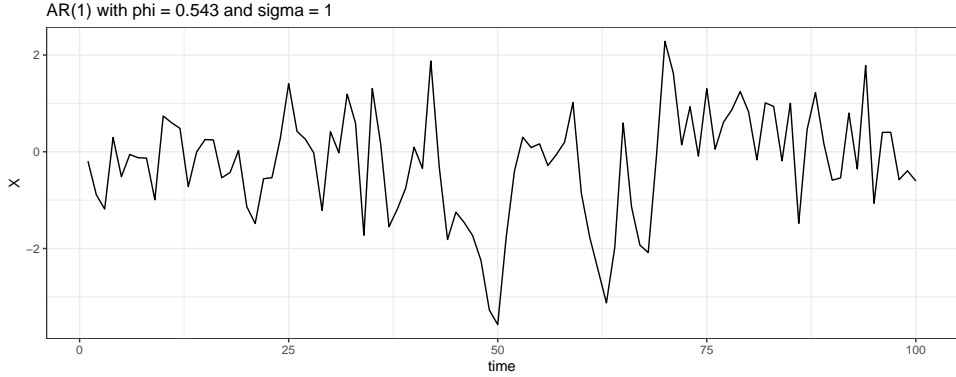


Figure 3: Whittle objective for the simulated series.

The maximiser occurs close to $\phi = 0.543$, agreeing with the ML fit.

(g)

We simulate $R = 300$ independent AR(1) samples with $\phi = 0.543$ for $n \in \{100, 500, 1000\}$ and compute ML and Whittle estimates. The empirical RMSEs are:

n	100	500	1000
RMSE($\hat{\phi}_{\text{ML}}$)	0.0870	0.0403	0.0271
RMSE($\tilde{\phi}_W$)	0.0910	0.0404	0.0270

Both estimators are nearly unbiased. The ML estimator is slightly more accurate at $n = 100$, but the difference vanishes as n increases, confirming asymptotic equivalence.

(h)

Under the exponential approximation for the periodogram,

$$-\frac{1}{n} \mathbb{E} \left[\frac{\partial^2}{\partial \phi^2} \ell_n^W(\phi) \right] = 4 \int_0^1 (\phi - \cos(2\pi u))^2 f(u, \phi)^2 du,$$

a positive finite limit. For the simulated sample (plugging in $\phi = 0.543$),

$$-\frac{1}{n} \frac{\partial^2}{\partial \phi^2} \ell_n^W(\phi) \approx 0.832,$$

which numerically agrees with the Fisher information of the exact Gaussian likelihood. Hence the Whittle estimator is asymptotically efficient for AR(1).

Exercise 3

Let $\{X_t\}$ be i.i.d. with mean μ_X and variance σ_X^2 , $\{W_t\}$ i.i.d. with mean 0 and variance σ_W^2 , independent of $\{X_t\}$. Let $\varepsilon_t = \phi\varepsilon_{t-1} + W_t$ with $|\phi| < 1$, and $Y_t = \alpha + \beta X_t + \varepsilon_t$. The OLS slope $\hat{\beta}_n$ satisfies

$$\sqrt{n}(\hat{\beta}_n - \beta) = \frac{n^{-1/2} \sum_{t=1}^n (X_t - \bar{X}_n) \varepsilon_t}{n^{-1} \sum_{t=1}^n (X_t - \bar{X}_n)^2}. \quad (2)$$

(a)

Let Z_1, \dots, Z_n be i.i.d. with $\mathbb{E}Z = 0$. For any $\varepsilon > 0$ and $K > 0$,

$$\mathbb{P}\left(\left|\frac{1}{n} \sum_{i=1}^n Z_i\right| \geq \varepsilon\right) \leq \frac{2}{\varepsilon} \mathbb{E}[|Z| \mathbf{1}\{|Z| \geq K\}] + \frac{4K}{\varepsilon^2} \cdot \frac{1}{n} \mathbb{E}|Z|.$$

Letting first $K \rightarrow \infty$ and then $n \rightarrow \infty$ yields the LLN: $n^{-1} \sum_i Z_i \xrightarrow{p} 0$. Apply with $Z_i = X_i - \mu_X$ to get $\bar{X}_n \xrightarrow{p} \mu_X$ and

$$\frac{1}{n} \sum_{t=1}^n (X_t - \bar{X}_n)^2 = \frac{1}{n} \sum_{t=1}^n (X_t - \mu_X)^2 - (\bar{X}_n - \mu_X)^2 \xrightarrow{p} \sigma_X^2.$$

Thus the denominator converges in probability to σ_X^2 .

(b)

Write

$$n^{-1/2} \sum_{t=1}^n (X_t - \bar{X}_n) \varepsilon_t = n^{-1/2} \sum_{t=1}^n (X_t - \mu_X) \varepsilon_t + \underbrace{\sqrt{n}(\mu_X - \bar{X}_n) \cdot \left(n^{-1} \sum_{t=1}^n \varepsilon_t\right)}_{r_n}.$$

By (a), $\sqrt{n}(\bar{X}_n - \mu_X) = O_p(1)$, and since $\{\varepsilon_t\}$ is stationary with mean 0, $n^{-1} \sum_t \varepsilon_t \xrightarrow{p} 0$. Hence $r_n \xrightarrow{p} 0$, so we may replace $(X_t - \bar{X}_n)$ by $(X_t - \mu_X)$ in the numerator.

(c)

Write $\varepsilon_t^{(m)} = \sum_{j=0}^m \phi^j W_{t-j}$. For fixed m , this is an m -dependent sequence, so $(X_t - \mu)\varepsilon_t^{(m)}$ is also m -dependent, mean zero and stationary. A standard CLT for m -dependent sequences then shows that the numerator of $\hat{\beta}_n$ has a \sqrt{n} -limit which is Normal. As $m \rightarrow \infty$ we recover the true AR(1) errors, and combining with the limit for the denominator gives

$$\sqrt{n}(\hat{\beta}_n - \beta) \xrightarrow{d} N\left(0, \frac{\sigma_W^2}{\sigma_X^2(1 - \phi^2)}\right).$$

This is a direct analogue of the usual OLS CLT with i.i.d. noise: if $\phi = 0$ (the errors are uncorrelated) the variance reduces to σ_W^2 / σ_X^2 , the standard linear regression result. When $\phi \neq 0$ the noise is serially correlated, so the asymptotic variance is inflated by the factor $1/(1-\phi^2)$. Intuitively: persistent errors make estimating β harder, so the estimator is more variable.

(d)

A consistent plug-in estimator of the asymptotic variance is

$$\widehat{\text{AVAR}}(\hat{\beta}_n) = \frac{\hat{\sigma}_W^2}{\hat{\sigma}_X^2 (1 - \hat{\phi}^2)},$$

where: (i) fit OLS $Y_t \sim \alpha + \beta X_t$ and compute residuals \hat{e}_t ; (ii) estimate $\hat{\phi}$ by regressing \hat{e}_t on \hat{e}_{t-1} ; (iii) set $\hat{\sigma}_W^2 = \frac{1}{n-1} \sum_{t=2}^n (\hat{e}_t - \hat{\phi} \hat{e}_{t-1})^2$; (iv) set $\hat{\sigma}_X^2 = \frac{1}{n} \sum_{t=1}^n (X_t - \bar{X}_n)^2$. A $(1 - \alpha)$ Wald CI for β is

$$\hat{\beta}_n \pm z_{1-\alpha/2} \sqrt{\frac{\widehat{\text{AVAR}}(\hat{\beta}_n)}{n}}.$$

Exercise 4

(a)

Figure 4 shows the downloaded EUR/NOK series. Fitting the AR(1) model $X_t = \phi X_{t-1} + W_t$ gives

$$\hat{\phi} = 0.9999598, \quad 95\% \text{ CI} = (0.9993914, 1.0005282).$$

The estimate is extremely close to 1, and the confidence interval contains 1. This indicates a highly persistent series, consistent with a random walk or near-unit-root behaviour.

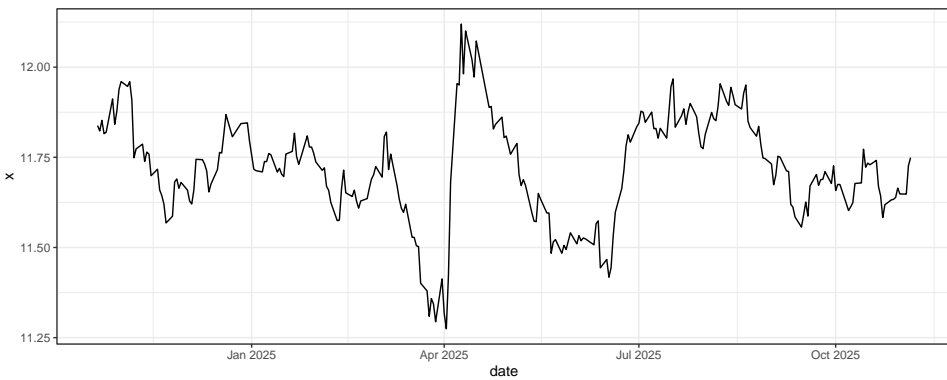


Figure 4: EUR/NOK spot series from Norges Bank API used for AR(1) estimation.

```
> phi; phi+c(-1,1)*qnorm(.975)*se
[1] 0.9999598
[1] 0.9993914 1.0005282
```

(b)

We test $H_0 : \phi = 1$ (random walk) versus $H_1 : |\phi| < 1$ (causal AR(1)) using the limit distribution in (3). The p-value obtained by simulation is

$$\Pr(|T_{\text{sim}}| \geq |T_{\text{obs}}|) = 0.993.$$

This is very large, so we do *not* reject H_0 . The data is entirely consistent with a random walk.

```
> mean(abs(Tsim)>=abs(Tobs))
[1] 0.993
```

(c)

Figure 5 compares the observed increments $X_t - X_{t-1}$ with simulated i.i.d. $W_t \sim N(0, \hat{\sigma}_n^2)$. Both series fluctuate around zero on a similar scale, but the empirical increments show clear volatility clustering, while the simulated Gaussian noise is more homogeneous. This again suggests that a simple i.i.d. noise model is not sufficient for the data.

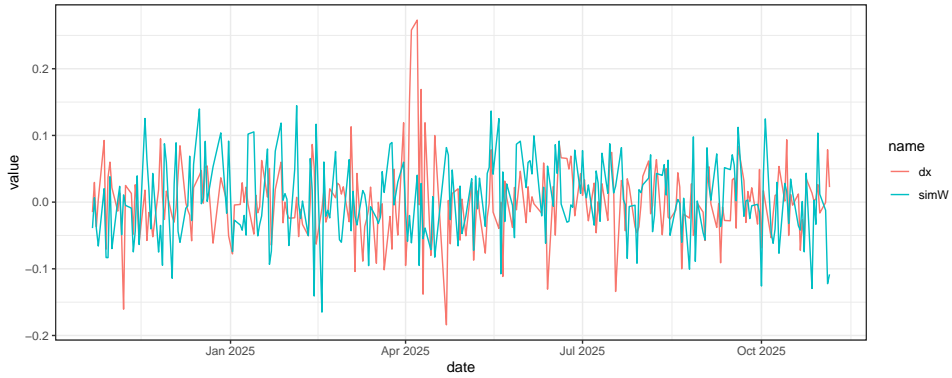


Figure 5: Observed increments $X_t - X_{t-1}$ (black) compared with simulated i.i.d. $N(0, \hat{\sigma}^2)$ noise (red). The real data shows volatility clustering, unlike the Gaussian noise.

(d)

We now consider the random-variance random walk model

$$X_t = X_{t-1} + \sigma_t W_t, \quad W_t \sim N(0, 1),$$

with $\lambda_t = 1/\sigma_t^2 \sim \text{Gamma}(\lambda_0/c, 1/c)$ i.i.d. The parameter c controls the variability of the σ_t^2 ; larger c gives heavier tails and more volatile increments. The likelihood based on $X_t - X_{t-1}$ for $t = 2, \dots, n$ is

$$L_n(\lambda_0, c) = (2\pi)^{-n/2} c^{-n\lambda_0/c} \frac{\Gamma(\lambda_0/c + 1/2)^n}{\Gamma(\lambda_0/c)^n} \prod_{t=2}^n \left(\frac{1}{c} + \frac{1}{2}(X_t - X_{t-1})^2 \right)^{-(\lambda_0/c+1/2)}.$$

(e)

Maximising the log-likelihood gives estimates $\hat{\lambda}_0$ and \hat{c} . Using these estimates, we simulate increments from the random-variance model. Figure 6 compares simulated data to the observed increments. The simulated increments display heavier tails and time-varying volatility, which visibly resembles the real data much better than the i.i.d. Gaussian noise from part (c).

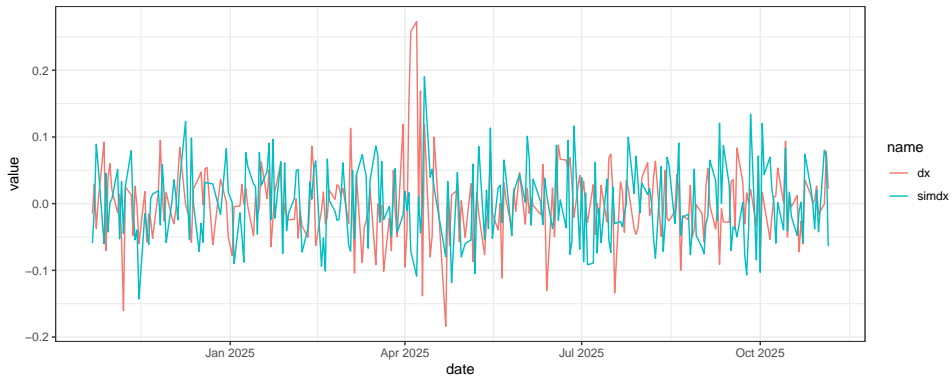


Figure 6: Observed increments $X_t - X_{t-1}$ (black) vs. simulated increments from the random-variance model (blue). The simulated series shows time-varying volatility and heavier tails, giving a much closer fit to the data.

(f)

Finally, we compare one-step-ahead predictions from the random-variance model to a simple random walk forecast. Using the last 60 observations, the empirical root mean squared errors are

$$\text{RMSE}_{\text{RW}} = 0.04004099, \quad \text{RMSE}_{\text{ARIMA}(0,1,1)} = 0.04011073.$$

The simple random walk achieves slightly lower prediction error. In this data set and period, a more complicated model does not improve short-term forecast accuracy.

```
> sqrt(mean((act-pred_rw)^2)); sqrt(mean((act-pred_ar)^2))
[1] 0.04004099
[1] 0.04011073
```

R-code

Exercise 1

```

1 library(tidyverse)
2 set.seed(4060)
3
4 # exercise 1
5
6 # a)
7
8 rho <- 0.4
9 n <- 100
10
11 Sigma <- outer(1:n, 1:n, function(t, s) rho^(abs(t - s)))
12
13 L <- chol(Sigma)
14 Z <- rnorm(n)
15 X <- as.vector(t(L) %*% Z)
16
17 acov_est <- acf(X, type = "covariance", plot = FALSE, lag.max = 3)$acf
18
19 tibble(
20   lag = 0:3,
21   empirical_autocov = as.numeric(acov_est)
22 )
23
24 # b)
25
26 rho <- 0.4
27 n <- 100
28 beta <- 0.05
29
30 Sigma <- outer(1:n, 1:n, function(t, s) rho^(abs(t - s)))
31
32 L <- chol(Sigma)
33 Z <- rnorm(n)
34 X <- as.vector(t(L) %*% Z)
35
36 t <- 1:n
37 Y <- beta * t + X
38
39 # theoretical autocovariance of Y: since beta*t is deterministic,
40 # Cov(Yt, Ys) = Cov(Xt, Xs) = rho^|t-s|
41
42 # plot Y_t
43 df_Y <- tibble(
44   time = t,
45

```



```

94 theory_gammaX <- rho^(0:3)
95 expected_acov <- det_term + theory_gammaX
96
97 tibble(
98   lag = 0:3,
99   empirical_autocov_Y = as.numeric(acov_Y),
100  deterministic_component = det_term,
101  gamma_X_theory = theory_gammaX,
102  expected_gammahat_Y = expected_acov
103 )
104
105 # d)
106
107 rho <- 0.4
108 n <- 100
109 beta <- 0.05
110
111 Sigma <- outer(1:n, 1:n, function(t, s) rho^(abs(t - s)))
112 L <- chol(Sigma)
113 Z <- rnorm(n)
114 X <- as.vector(t(L) %*% Z)
115
116 t <- 1:n
117 Y <- beta * t + X
118
119 # detrend: Y*_t = Y_t - beta*t
120 Y_star <- Y - beta * t
121
122 acov_Y_star <- acf(Y_star, type = "covariance", plot = FALSE, lag =
123   max = 3)$acf
124
125 tibble(
126   lag = 0:3,
127   empirical_autocov_Ystar = as.numeric(acov_Y_star)
128 )

```

Exercise 2

```

1 library(tidyverse)
2 set.seed(4060)
3
4 # exercise 2
5
6
7 # a)
8
9 phi <- 0.543
10 n <- 100
11 burn <- 200

```

```

12 W <- rnorm(n + burn)
13 X <- numeric(n + burn)
14 X[1] <- rnorm(1, sd = 1 / sqrt(1 - phi^2))
15
16 for (t in 2:(n + burn)) {
17   X[t] <- phi * X[t - 1] + W[t]
18 }
19
20 X <- X[(burn + 1):(burn + n)]
21
22 df_X <- tibble(
23   time = 1:n,
24   X = X
25 )
26
27 p <- ggplot(df_X, aes(time, X)) +
28   geom_line() +
29   theme_bw() +
30   labs(title = "AR(1) with phi = 0.543 and sigma = 1")
31
32 ggsave("plots/ar1_phi543.pdf", p, width = 12, height = 6)
33
34 df_X
35
36
37
38 # b)
39
40 loglik <- function(phi, X) {
41   n <- length(X)
42   term1 <- 0.5 * log(1 - phi^2)
43   term2 <- -0.5 * (1 - phi^2) * X[1]^2
44   term3 <- -0.5 * sum((X[2:n] - phi * X[1:(n-1)])^2)
45   term1 + term2 + term3
46 }
47
48 score <- function(phi, X) {
49   n <- length(X)
50   part1 <- -phi / (1 - phi^2)
51   part2 <- X[1]^2 * phi
52   part3 <- sum((X[2:n] - phi * X[1:(n-1)]) * X[1:(n-1)])
53   part1 + part2 + part3
54 }
55
56 Jn <- function(phi, X) {
57   n <- length(X)
58   s2 <- sum(X[1:(n-1)]^2)
59   part1 <- -(1 + phi^2) / (1 - phi^2)^2
60   part2 <- -sum(X[1]^2)
61   part3 <- -s2
62   -(1/n) * (part1 + part2 + part3)

```

```

63 }
64
65 loglik(phi, X)
66 score(phi, X)
67 Jn(phi, X)
68
69
70 # c)
71
72 meansq <- cumsum(X^2) / (1:n)
73 tail(meansq, 5)
74
75
76 # e)
77
78 f_ar1 <- function(w, phi) {
79   (1/(2*pi)) / (1 + phi^2 - 2*phi*cos(2*pi*w))
80 }
81
82 whittle <- function(phi, x){
83   n <- length(x)
84   j <- 1:floor((n-1)/2)
85   w <- j/n
86   dx <- fft(x) / sqrt(n)
87   Iw <- Mod(dx[j+1])^2
88   sum(log(f_ar1(w,phi)) + Iw / f_ar1(w,phi))
89 }
90
91 # f)
92
93 phis <- seq(-0.95, 0.95, by=0.01)
94 vals <- sapply(phis, whittle, x=X)
95 plot(phis, -vals, type="l")
96 ggsave("plots/whittle_curve.pdf", width=10, height=4)
97
98 # g)
99
100 sim_compare <- function(n, R=300, phi=0.543){
101   rmse <- function(est) sqrt(mean((est - phi)^2))
102
103   ml <- wh <- numeric(R)
104   for(r in 1:R){
105     W <- rnorm(n+200)
106     Z <- numeric(n+200)
107     Z[1] <- rnorm(1, sd = 1/sqrt(1-phi^2))
108     for(t in 2:(n+200)) Z[t] <- phi*Z[t-1]+W[t]
109     x <- Z[(200+1):(200+n)]
110
111     ml[r] <- optimize(function(a) -loglik(a, x), c(-0.99, 0.99))$minimum

```

```

112     wh[r] <- optimize(function(a) whittle(a, x), c(-0.99, 0.99))$minimum
113   }
114   c(RMSE_ML = rmse(ml), RMSE_Whittle = rmse(wh))
115 }
116
117 sim_compare(100)
118 sim_compare(500)
119 sim_compare(1000)
120
121 # h)
122
123 curv <- function(phi) {
124   j <- 1:floor((n-1)/2)
125   w <- j/n
126   sum( (phi - cos(2*pi*w))^2 * f_ar1(w, phi)^2 )
127 }
128 curv(phi)

```

Exercise 4

```

1 library(tidyverse)
2 library(readr)
3
4
5 eur_link <- "https://data.norges-bank.no/api/data/EXR/B.EUR.NOK.SP?"
6   format=csv&bom=include&apisrc=nbi&startPeriod=2024-10-21&locale=
7   no"
8 eur <- read_csv2(eur_link, locale = locale(decimal_mark=","),
9   col_types = FALSE) %>% arrange(TIME_PERIOD)
10
11 xx <- eur %>% pull(OBS_VALUE)
12 n <- length(xx)
13
14 # a)
15 df <- tibble(date=eur$TIME_PERIOD, x=xx)
16 ggplot(df,aes(date,x))+geom_line()+theme_bw()
17 ggsave("plots/a.pdf",width=10,height=4)
18 phi <- sum(xx[-n]*xx[-1])/sum(xx[-n]^2)
19 s2 <- mean((xx[-1]-phi*xx[-n])^2)
20 se <- sqrt(s2/sum(xx[-n]^2))
21 phi; phi+c(-1,1)*qnorm(.975)*se
22
23 # b)
24 set.seed(4060)
25 Tobs <- n*(phi-1)
26 sim <- function(M=4000,m=2000){
27   Z<-matrix(rnorm(M*m,0,1/sqrt(m)),M);B<-t(apply(Z,1,cumsum))
28 }
```

```

26 int<-rowMeans(B^2);T<-0.5*(rchisq(M,1)-1)/int;T}
27 Tsim <- sim()
28 mean(abs(Tsim)>=abs(Tobs))

29
30 # c)
31 dx <- diff(xx); s2dx <- var(dx)
32 simW <- rnorm(length(dx),sd=sqrt(s2dx))
33 tibble(date=df$date[-1],dx,simW) %>%
34   pivot_longer(-date) %>%
35   ggplot(aes(date,value,color=name))+geom_line()+theme_bw()
36 ggsave("plots/c.pdf",width=10,height=4)

37
38 # d) e)
39 ll <- function(p){
40   10<-exp(p[1]);c<-exp(p[2]);k<-10/c;r<-1/c
41   sum(-(k+.5)*log(1/c+.5*dx^2))+(-length(dx)/2)*log(2*pi)-length(dx)
42   *(10/c)*log(c)+
43   length(dx)*(lgamma(k+.5)-lgamma(k))}
44 o<-optim(c(0,log(.2)),function(p)-ll(p))
45 10<-exp(o$par[1]);c<-exp(o$par[2]);k<-10/c;r<-1/c
46 lam<-rgamma(length(dx),k,r);sdv<-1/sqrt(lam)
47 simdx<-rnorm(length(dx),sd=sdv)
48 tibble(date=df$date[-1],dx,simdx) %>%
49   pivot_longer(-date) %>%
50   ggplot(aes(date,value,color=name))+geom_line()+theme_bw()
51 ggsave("plots/e.pdf",width=10,height=4)

52 # f)
53 h<-60
54 r wf<-xx[(n-h):(n-1)]
55 pred_rw<-xx[(n-h):(n-1)]
56 pred_ar<-map_dbl((n-h+1):n,function(t) as.numeric(predict(arima(xx
57   [1:(t-1)],c(0,1,1)),1)$pred)))
58 act<-xx[(n-h+1):n]
59 sqrt(mean((act-pred_rw)^2)); sqrt(mean((act-pred_ar)^2))

```